Surgical Oncology 29 (2019) 148–156

Contents lists available at ScienceDirect

Surgical Oncology

journal homepage: www.elsevier.com/locate/suronc

Local treatment of liver metastases by administration of ^{177}Lu-octreotate via isolated hepatic perfusion – A preclinical simulation of a novel treatment strategy

Viktor Sandblom[a,*], Ingun Ståhl[a], Christoffer Hansson[b], Roger Olofsson Bagge[c,d,e], Eva Forssell-Aronsson[a,f]

[a] Department of Radiation Physics, Institute of Clinical Sciences, Sahlgrenska Cancer Center, Sahlgrenska Academy, University of Gothenburg, SE-413 45, Gothenburg, Sweden
[b] Department of Cardiothoracic Surgery, Sahlgrenska University Hospital, SE-413 45, Gothenburg, Sweden
[c] Department of Surgery, Institute of Clinical Sciences, Sahlgrenska Academy, University of Gothenburg, SE-413 45, Gothenburg, Sweden
[d] Department of Surgery, Sahlgrenska University Hospital, SE-413 45, Gothenburg, Sweden
[e] Wallenberg Centre for Molecular and Translational Medicine, University of Gothenburg, SE-413 45, Gothenburg, Sweden
[f] Department of Medical Physics and Biomedical Engineering, Sahlgrenska University Hospital, SE-413 45, Gothenburg, Sweden

ARTICLE INFO

Keywords:
Isolated hepatic perfusion
Neuroendocrine tumour
Somatostatin receptor
PRRT
Intraoperative gamma detector
Pig

ABSTRACT

Introduction: Systemic ^{177}Lu-octreotate treatment for metastatic neuroendocrine tumours is restricted by organs at risk. By administering ^{177}Lu-octreotate during isolated hepatic perfusion (IHP), the uptake in organs at risk might be strongly reduced. The aim of this study was to investigate the feasibility to use the combination of IHP and radionuclide therapy.

Methods: To simulate IHP, the liver of a pig was prepared for *ex vivo* perfusion. Blood containing 490 MBq ^{177}Lu-octreotate was circulated through the liver for 60 min, after which the liver was rinsed. After IHP, the liver was examined by SPECT/CT. Lastly, an intraoperative gamma detector (IGD) was used to determine ^{177}Lu activity concentration in the liver and results were compared with the activity concentration in corresponding liver biopsies.

Results: Detector measurements over the liver during the IHP showed a fast increase with a maximum after approximately 10–15 min. After IHP, about 75% of the ^{177}Lu in the liver could be washed out. The SPECT/CT images revealed a relatively inhomogeneous distribution. Nevertheless, the IGD values of ^{177}Lu activity concentration showed acceptable agreement with the biopsy values.

Conclusions: Our results in pig show that it could be feasible to treat patients with liver metastases from NETs with ^{177}Lu-octreotate via IHP ^{177}. However, an inhomogeneous distribution of ^{177}Lu-octreotate in normal liver tissue is expected, and in order to determine the activity concentration with satisfactory accuracy using an IGD, measurements need to be performed at several positions over the liver.

1. Introduction

Neuroendocrine tumours (NETs) are a group of heterogeneous slow-growing tumours that have their origin in hormone producing organs [1–3]. In the United States, the incidence of NETs has increased over the past few decades from about 1 to 5 cases per 100,000 people, and is expected to reach 8 per 100,000 today. Because of the vague symptoms of these tumours and their slow growth rate, patients with NETs are often diagnosed after the primary tumour has already metastasised. Therefore, patients with NETs are difficult to cure and reported values of 5-year survival in the literature vary between about 50 and 80%, depending on type of NET, clinical stage and treatment [2,4–8]. The most common site of origin for NETs is the gastrointestinal tract. Primary tumours of this region are likely to spread to the liver, and for patients with liver metastases, the survival rate is lower. For liver-dominant disease, several image-guided regional treatment methods are well-established, *e.g. trans*-arterial embolisation (TAE), *trans*-arterial chemoembolisation (TACE), and radioembolisation (RE). Another

* Corresponding author. Department of Radiation Physics, Gula Stråket 2B, SE-413 45, Gothenburg, Sweden.
E-mail addresses: viktor.sandblom@gu.se (V. Sandblom), ingun.stahl@gu.se (I. Ståhl), christoffer.hansson@vgregion.se (C. Hansson), roger.olofsson@gu.se (R. Olofsson Bagge), eva.forssell_aronsson@radfys.gu.se (E. Forssell-Aronsson).

https://doi.org/10.1016/j.suronc.2019.05.002
Received 9 November 2018; Received in revised form 17 April 2019; Accepted 10 May 2019
0960-7404/ © 2019 The Authors. Published by Elsevier Ltd. This is an open access article under the CC BY-NC-ND license (http://creativecommons.org/licenses/BY-NC-ND/4.0/).

Abbreviations

CT	computed tomography
CV	coefficient of variation
FOV	field-of-view
IGD	intraoperative gamma detector
IHP	isolated hepatic perfusion
NET	neuroendocrine tumour
PRRT	peptide receptor radionuclide therapy
RE	radioembolisation
SD	standard deviation
SEM	standard error of the mean
SPECT	single-photon emission computed tomography
SSTR	somatostatin receptor
TACE	*trans*-arterial chemoembolisation
TAE	*trans*-arterial embolisation

option is liver or multivisceral transplantation [9]. General treatment methods for disseminated NETs include the use of somatostatin analogues, interferon-alpha, chemotherapy, and targeted therapies, *e.g.* radionuclide therapy [10–13]. The most common radionuclide therapy for metastatic NETs today is systemic treatment with the radiolabelled somatostatin analogue ^{177}Lu-octreotate that binds to somatostatin receptors (SSTRs) expressed by the tumour tissue. This treatment type is also called peptide receptor radionuclide therapy (PRRT). Even though it has shown very promising results, the possibility of complete cure may be restricted by the absorbed dose to organs at risk, mainly kidneys and red bone marrow [14–19]. There is a need for optimisation of this treatment method and the two main options that exist are to 1) reduce the side effects on organs at risk or to 2) increase the effect on the tumour tissue [20].

Isolated hepatic perfusion (IHP) is a treatment technique in which the liver is completely isolated from the systemic circulation, allowing high doses of drugs to be administered locally to the liver with minimal systemic exposure [21–23]. Briefly, a percutaneous bypass from the lower extremity is created around the liver by connecting the femoral and the external jugular vein to a pump. The liver is then completely mobilised, the portal vein is clamped and the hepatic artery and the inferior caval vein is cannulated and connected to an oxygenated perfusion system, *i.e.* a heart-lung machine. This setup creates an isolated circuit in which a certain blood volume can be continuously circulated through the liver. Drugs can then be administered directly into the perfusion circuit passing through the liver with minimal systemic leakage and risk for toxicity. After 60 min, the liver is rinsed with crystalloid fluid and the treatment is completed by the restoration of the normal systemic circulation. IHP with the chemotherapeutic drug melphalan is commonly used to treat liver metastases from malignant melanoma and colorectal cancer, but has also been evaluated for NETs [24,25].

By administering ^{177}Lu-octreotate during IHP instead of systemically, the uptake in organs at risk, *e.g.* kidneys and bone marrow, might be strongly reduced. The administered amount of ^{177}Lu-octreotate may also be increased, resulting in higher absorbed dose to tumour tissue. However, one healthy organ that would not be unaffected by a large increase in the administered amount of activity is the liver itself. Therefore, when applying this strategy clinically, it will be important to be able to accurately monitor the ^{177}Lu activity concentration in healthy liver tissue *in vivo* during IHP in order to determine the absorbed dose accurately, and end the perfusion if needed to avoid late side effects. Based on a previous phantom study, we suggest that this could be done using an intraoperative gamma detector (IGD) [26]. Normally, such detectors are used diagnostically for radioguided surgery, during which a tumour-seeking radioactive tracer (low radioactivity) helps the surgeon to locate small possible lesions before removal [27]. One early example is the location of NETs, both primary tumours and liver and lymph node metastases, using ^{111}In-octreotide [28–31]. Another example is the location of sentinel lymph nodes using ^{99m}Tc-labelled sulphur colloid during breast cancer surgery [32,33]. Clinically, "diagnostic" radionuclides have mainly been used, *i.e.* radionuclides emitting high amounts of photons of relatively low energy. In the present application, a "therapeutic" radionuclide should be used, *i.e.* a radionuclide that emits low amounts of photons. This is, however, not a drawback in this application. Since high amounts of activity most probably will be used, a high photon emission yield could lead to detection problems due to dead-time effects (due to a too high count rate).

The aims of the present study were to study the feasibility to use ^{177}Lu-based radionuclide therapy by IHP by: 1) investigating whether an intraoperative gamma detector can be used to determine ^{177}Lu activity concentration in the liver, 2) investigating uptake and distribution of ^{177}Lu-octreotate in healthy liver tissue after administration during IHP, and 3) evaluating the radiation exposure situation for the staff involved in such a procedure. The study was performed using the liver of a pig in order to reasonably simulate a clinical situation.

2. Material and methods

2.1. Radiopharmaceutical

^{177}Lu-octreotate was ordered from IDB Holland (IDB Holland BV, Baarle-Nassau, the Netherlands) and prepared according the instructions of the manufacturer. The peptide bound fraction of the ^{177}Lu was determined to over 99% by instant thin layer chromatography (ITLC SG, PALL Corporation, USA) with the mobile phase consisting of 0.1 M sodium citrate (pH 5; VWR International AB, Spånga, Sweden). The syringe containing ^{177}Lu-octreotate was measured in a well-type ionisation chamber (CRC-15R, Capintec, Ramsey, New Jersey, USA) before and after administration to determine the amount of radioactivity used for the study.

2.2. Isolated hepatic perfusion with ^{177}Lu-octreotate in pig

To simulate a clinical situation involving a patient undergoing ^{177}Lu-octreotate treatment for liver metastases from NETs using the IHP technique, a healthy three month old pig (35 kg) was prepared for surgery. To avoid risk of even a potential very low contamination of the entire pig with ^{177}Lu (*i.e.* to avoid logistic problems caused by institutional rules for handling of the carcass after the experiment), the IHP procedure simulation was performed *ex vivo*. The liver was connected to a heart-lung machine in accordance with our standard IHP procedure with the exception that the hepatic artery was clamped instead of the portal vein, and the portal vein was cannulated and connected to an oxygenated perfusion system [23]. When the perfusion circuit had been established, the liver was removed and placed in a bowl, and the pig was euthanised. A blood reservoir was used as a buffer for the circulating blood. This reservoir was sealed in a 10 mm thick protective lead cylinder with a lead lid to minimise radiation exposure of the staff. In addition, the circuit contained an injection port to enable safe administration of substances into the blood reservoir (Fig. 1).

Once a steady blood flow of 150 ml/min had been established, 490 MBq ^{177}Lu-octreotate was added to the system via the injection port into the blood reservoir. During the perfusion, a small degree of leakage from the liver into the bowl was experienced (about 5 ml/min). This fluid, containing ^{177}Lu, was removed every 10 min in order not to interfere with the activity concentration measurements described below. At these times, Ringer's solution (Ringer Acetat, Baxter Medical AB, Kista, Sweden) was added directly into the blood reservoir in the

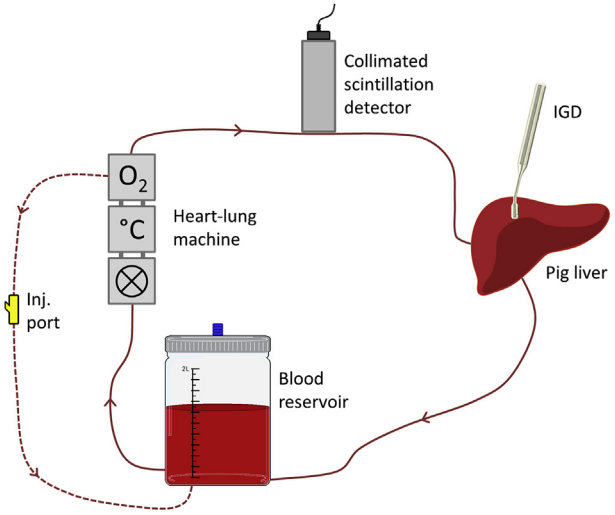

Fig. 1. Schematic view of the *ex vivo* isolated hepatic perfusion (IHP) circuit used for the study. The heart-lung machine consisted of a pump, a heat exchanger, and an oxygenator. The blood reservoir was sealed inside a 10 mm thick protective lead cylinder with a lead lid (not shown in figure). Two detectors were used to monitor the activity concentration – a collimated scintillation detector was placed over the tube transporting blood to the liver, and an intraoperative gamma detector (IGD) was placed over the thickest part of liver [single-column fitting image].

corresponding amount to compensate for the loss of fluid. After 60 min, the perfusion was stopped and the liver was disconnected from the perfusion circuit and rinsed with 9000 ml of Ringer's solution. This study was approved by the Ethical Committee on Animal Experiments in Gothenburg, Sweden.

Before ^{177}Lu-octreotate was added to the heart-lung machine's blood circulation system, two detectors were positioned to monitor the radioactivity concentration in the circulation system and in the liver, respectively. To measure ^{177}Lu activity concentration in the blood during the perfusion, a collimated NaI(Tl) scintillation detector (Scintibloc type 51 SL 12 no. 7775, Saint-Gobain S.A., La Défense, Courbevoie, France) connected to a computer with a locally developed analysing software (MedicView, Systemdata, Gothenburg, Sweden) was positioned over the circuit tube leading blood from the heart-lung machine to the liver. For this detector, an open energy window (about 50–3000 keV) was used to include the 113 keV and 208 keV photons, with an emission yield of 6.2% and 10%, respectively [34]. To measure activity concentration in the liver during the perfusion and rinsing, a small intraoperative CdTe semiconductor gamma detector (Navigator GPS with the probe model "Standard lymphatic mapping", Dilon Diagnostics, Newport News, Virginia, USA) with a ± 20% energy window centred over the ^{99m}Tc energy peak at 141 keV (range 112–169 keV) was positioned over the thickest part of the liver (approximately 7 cm). Both the scintillation detector and the IGD registered radiation as count rate.

2.3. SPECT/CT imaging

After the liver had been disconnected from the perfusion circuit and rinsed with Ringer's solution, it was examined by a clinical SPECT/CT system (Discovery NM/CT 670, GE Healthcare, Little Chalfont, United Kingdom) equipped with a medium-energy collimator. A ± 10% energy window centred over the 208 keV ^{177}Lu peak was used to collect 120 projection images with a collection time of 45 s per projection. The projection images were reconstructed with attenuation correction into a stack of 128 SPECT images with 128x128 pixels, and voxel size 86 mm^3. In addition, the liver was imaged with the CT scanner (tube voltage 120 kV, tube current 220 mA). The images were reconstructed with a slice thickness of 3.75 mm. Fused SPECT/CT images were analysed

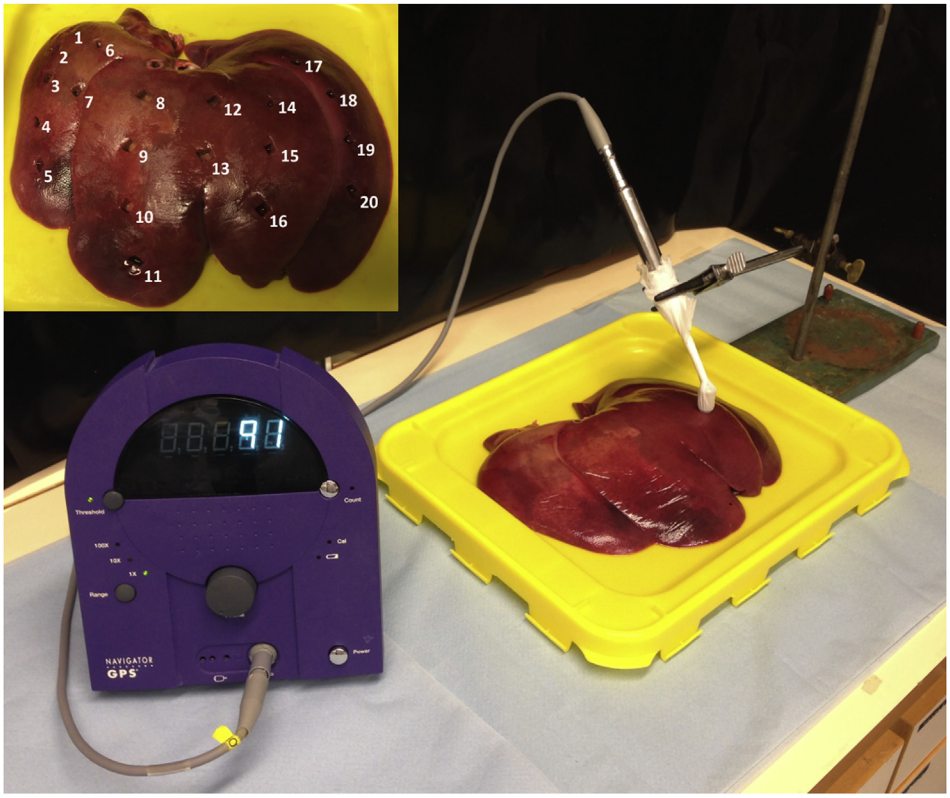

Fig. 2. Measurement setup for the intraoperative gamma detector (IGD) measurements with subsequent biopsy sampling at 20 positions, performed after the *ex vivo* isolated hepatic perfusion (IHP) [single-column fitting image].

using Xeleris Workstation (GE Healthcare, Little Chalfont, United Kingdom).

2.4. IGD measurements vs. biopsies

In order to investigate the ability and accuracy of the IGD to determine ^{177}Lu activity concentration in the liver, additional post-IHP measurements of activity concentration were made with the IGD and compared with the activity concentration in liver biopsies. The IGD probe (covered with thin plastic to avoid contamination) was placed in direct contact with the liver surface and the count rate was measured, followed by sampling of a biopsy (about $1 \times 1 \times 1\ cm^3$) in the same location. This was repeated for 20 locations over the liver (Fig. 2). The liver thickness in each position was estimated using a ruler.

The measured count rate by the IGD was translated into an activity concentration using calibration data from a previously published study [26]. In that study, we used an agarose gel phantom, containing a known homogenous activity concentration of ^{177}Lu, to simulate liver tissue. Using the same IGD, the count rate at the surface of different thicknesses of this agarose liver phantom was measured. Then, using the count rate measured in this study, the activity concentration, C_{IGD}, was estimated for each position:

$$C_{IGD} = \frac{R_L(x)}{R_P(x)} \times C_P, \quad (1)$$

where $R_L(x)$ was the count rate measured over the liver at a thickness x, $R_P(x)$ was the count rate measured over the agarose gel phantom at the same thickness x, and C_P was the known activity concentration in the agarose gel phantom.

The liver biopsies were weighed and the activity was measured by a calibrated gamma counter (Wallac 1480 Wizard 3", Wallac Oy, Turku, Finland), and the activity concentration, C_B, was determined. The gamma counter used an energy window over the 208 keV peak, and was calibrated against the well-type ionisation chamber. Corrections were made for background signal and dead-time effects. All activity concentration values were corrected for radioactive decay to the time of ^{177}Lu-octreotate administration during the IHP.

In order to further evaluate the homogeneity of the ^{177}Lu-octreotate distribution in the liver (in addition to the SPECT/CT data), 30 extra biopsies were taken from the liver tissue and measured in the gamma counter.

2.5. Radiation exposure of staff

All three staff members present in the animal laboratory operating room after ^{177}Lu had been added to the perfusion circuit wore personal dosimeters (Harshaw TLD, Thermo Scientific, Waltham, Massachusetts, USA), both for whole body exposure ($H_p(10)$) worn on the torso and for extremity exposure ($H_p(0.07)$) worn around the arm wrist. The exposure environment, as H*(10), was also evaluated by measurements with a hand-held intensimeter (RNI 10/SR Intensimeter, Nuklidtech Sweden AB, Jordbro, Sweden) at locations in the room where high radiation dose was expected – close to the blood reservoir and at the surface of the liver.

3. Results

The ^{177}Lu activity content measured over the circuit tube and over the liver during the perfusion with ^{177}Lu-octreotate and rinsing with Ringer's solution is presented in Fig. 3. The IGD measurements over the liver showed a fast increase in count rate with a maximum approximately 10–15 min after the ^{177}Lu-octreotate was added to the perfusion circuit, followed by a slow decrease in count rate during the rest of the perfusion period. About 75% of the ^{177}Lu was washed out by the Ringer's solution.

The ^{177}Lu activity concentration values in the liver tissue obtained with the IGD showed overall good agreement with the corresponding values for the biopsies (Pearson's $r = 0.714$ and $p < 0.001$) (Fig. 4). The C_{IGD}/C_B values ranged from 0.54 to 1.45, with a mean value of 0.93 and a SEM of 0.06. Furthermore, the C_{IGD}/C_B ratio increased with

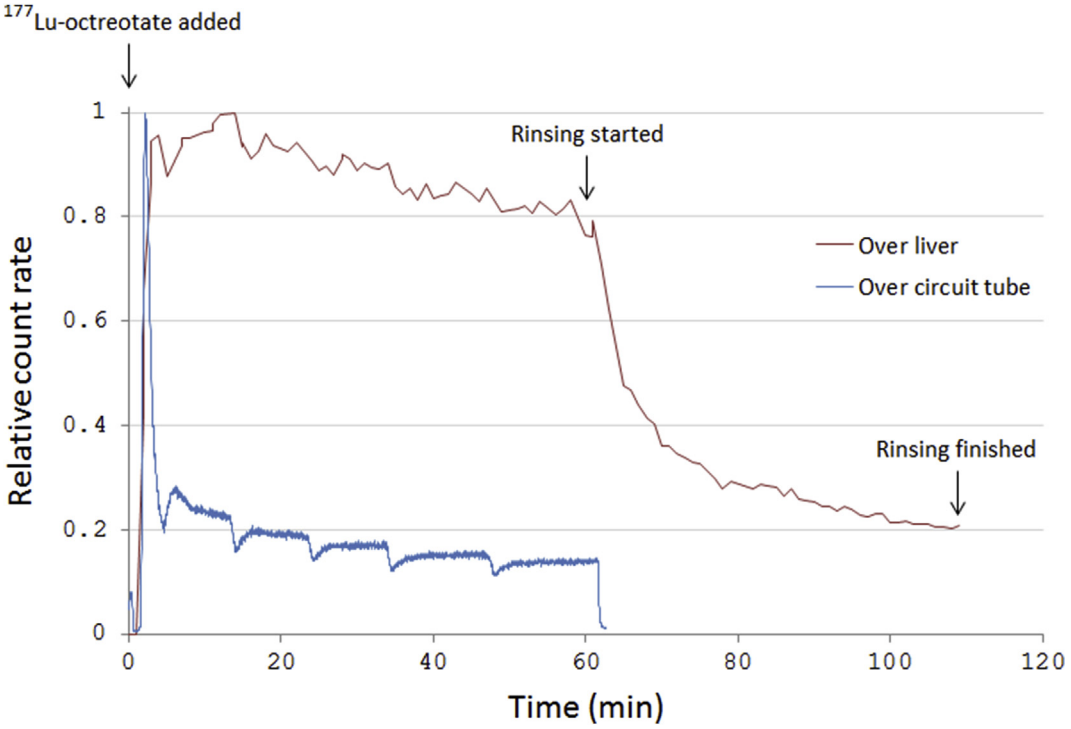

Fig. 3. Time dependence of the activity content presented as relative count rate, i.e. the count rate measured with each detector normalised to the highest count rate measured with the same detector. The ^{177}Lu-octreotate was added at time 0 min and the rinsing with Ringer's solution started after 60 min and finished at time 109 min [single-column fitting image].

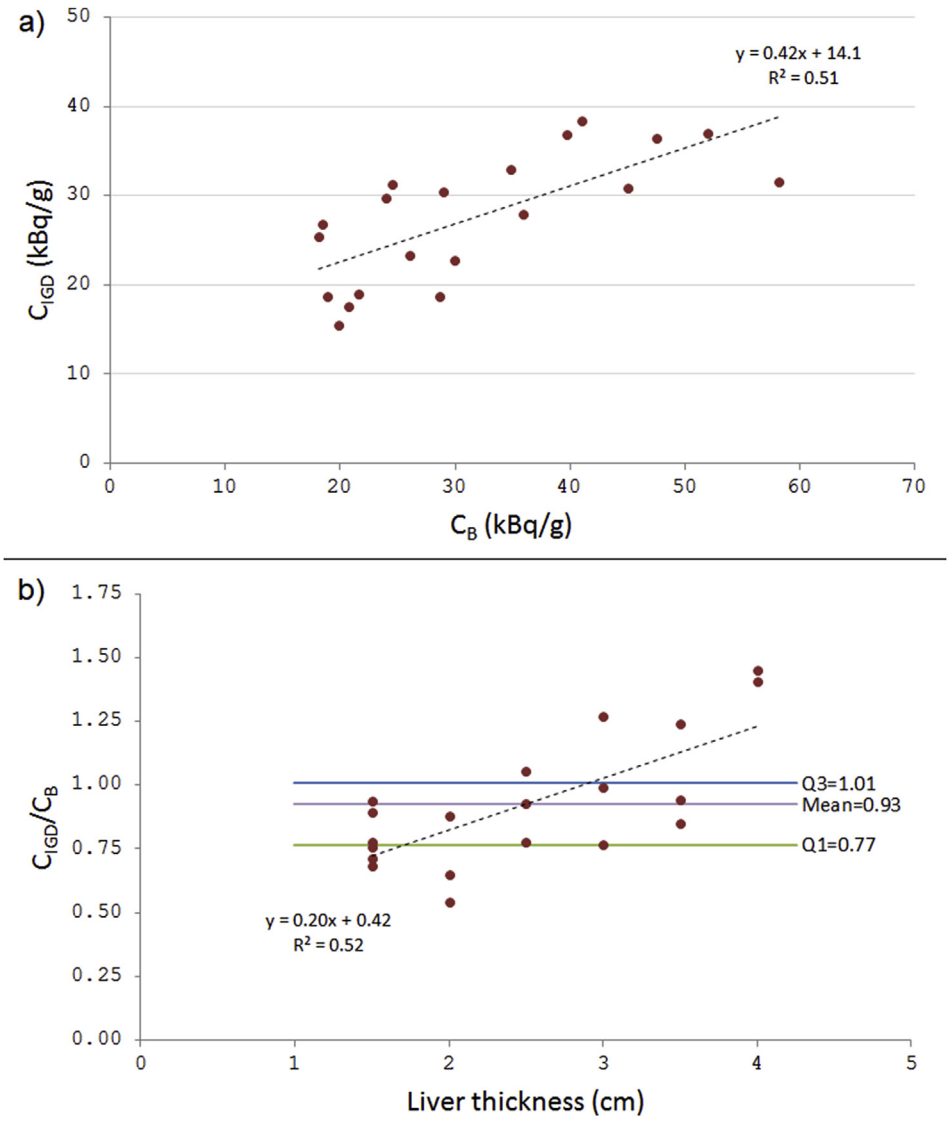

Fig. 4. Comparison between the ^{177}Lu activity concentration estimated by the intraoperative gamma detector (C_{IGD}) and that in the corresponding biopsy (C_B) for the 20 positions shown in Fig. 2. In part a) C_{IGD} is plotted vs. C_B for each measurement position. In part b) the ratio (C_{IGD}/C_B) is plotted vs. liver thickness at the given measurement position, along with horizontal lines corresponding to the first quartile (Q1), mean and third quartile (Q3). R^2 is the coefficient of determination [single-column fitting image].

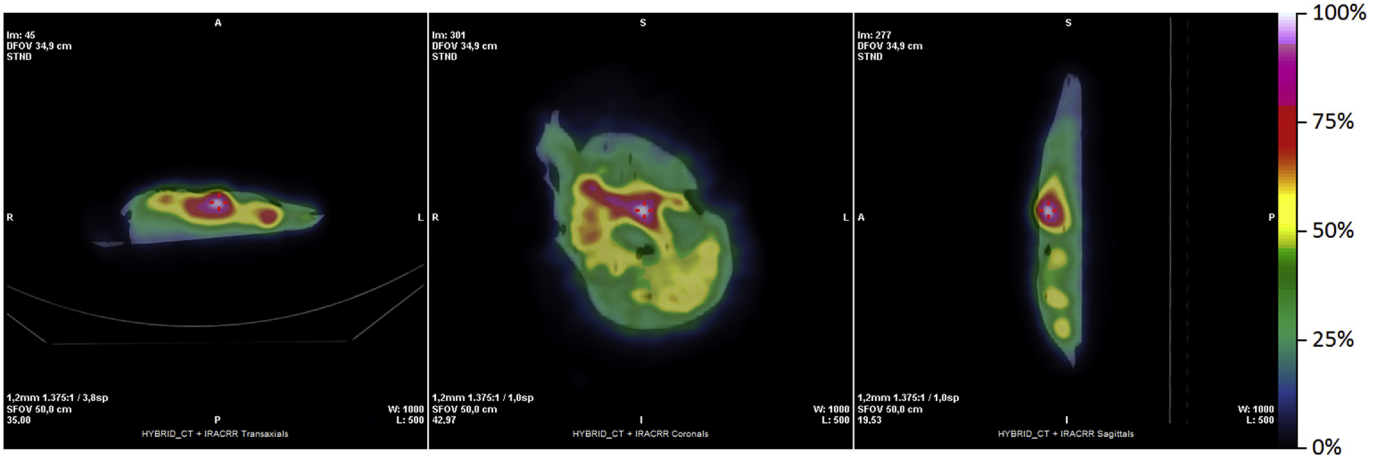

Fig. 5. Fused SPECT/CT images of the liver, acquired after the perfusion (490 MBq ^{177}Lu-octreotate) and rinsing had been finished, showing three different cross sections of the voxel with the highest voxel value (indicated by the red cross). The SPECT image was reconstructed using 120 projection images with a collection time of 45 s per projection [2-column fitting image].

increasing liver thickness.

The fused SPECT/CT image of the liver, acquired after rinsing, revealed a relatively inhomogeneous distribution of ^{177}Lu (Fig. 5). Analysing all voxels in the SPECT image with a value larger than 0 (n = 21087), the range of voxel values (*i.e.* counts per voxel) was 45–1500 with a mean value of 340 with a coefficient of variation (CV = SD/mean) of 77% and a SEM/mean of 0.53%. The activity concentration in the 50 biopsies taken from the liver can be seen in Fig. 6. The range of the activity concentration values was 18–79 kBq/g with a mean value of 39 kBq/g with a CV of 36% and a SEM/mean of 5.1%.

None of the personal dosimeters gave any measurable radiation dose at readout. The highest ambient equivalent dose rate measured with the intensimeter was 100 μSv/h at the surface of the liver. The corresponding values at 20 cm and 50 cm from the surface of the liver were 10 μSv/h and 4 μSv/h, respectively. The dose rate at the outer surface of the lead cylinder with lid containing the blood reservoir was at the same level as the background dose rate.

4. Discussion

In the present study, we examined the possibility to use ^{177}Lu-based therapy by IHP clinically by simulation in a pig model. The experiments were performed *ex vivo* for logistic reasons, as presented above, but based on previous experience of the IHP technique and intraoperative measurements, we believe that the data can readily be translated to a clinical situation.

The idea of local treatment of neuroendocrine liver metastases is not new. As previously mentioned, several intra-arterial therapies are well-established, *e.g.*TAE, TACE, and RE [35]. Another example is local administration of ^{90}Y-lanreotide by intra-arterial injection directly into the liver [36]. However, all these techniques differ substantially from our new treatment technique in that during these previously used treatments, drugs are administered with the normal blood circulation intact. In contrast, we propose the combined use of ^{177}Lu-octreotate and IHP, which means that the liver would be completely disconnected from the rest of the circulation system during treatment, leading to minimal uptake and exposure of the main organs at risk associated with ^{177}Lu-octreotate treatment, *i.e.* kidneys and bone marrow. To result in the same low expose of organs at risk, an intra-arterial administration would need practically 100% uptake of ^{177}Lu-octreotate in the liver metastases at first passage, something that is not realistic, demonstrated by pharmacokinetic data.

Healthy liver tissue consists of mainly of hepatocytes (parenchymal cells), but also of non-parenchymal cells, namely endothelial cells, phagocytic Kupffer cells, stellate cells and intrahepatic lymphocytes. The gamma detector measurements during the IHP showed a fast increase in count rate in the liver (Fig. 3). The maximum count rate was reached as early as 10–15 min after the administration of ^{177}Lu-octreotate. Since neither hepatocytes nor stellate cells in healthy human liver express SSTRs [37], the activity concentration in the liver was expected to increase over the course of the IHP until a homogeneous distribution in the extracellular space was obtained. The fast maximum obtained in this study supports that there was no receptor uptake, or that all receptors, if any, were immediately saturated, with a slow receptor turnover. The small decrease in activity concentration during the rest of the perfusion could be explained by dilution due to the added non-radioactive Ringer's solution that compensated for the loss in fluid. The five sudden small decreases in count rate (followed by rapid increases back to normal) measured over the circuit tube can also be explained by the added Ringer's solution.

After the liver had been rinsed with Ringer's solution, approximately 25% of the ^{177}Lu remained in the liver. One contributing factor for this is difficulties in achieving a sufficient rinsing in all parts of the liver, which is also supported by the large intensity variation in the SPECT images. A similar situation is seen for isolated limb perfusion treatments with melphalan (using the same principle of IHP), where a small part of the drug remains in the treatment region after rinsing [38]. The mechanisms of insufficient liver rinsing are not known but could be rheological, anatomic, or biochemical. Another factor could be that a certain part of the ^{177}Lu-octreotate molecules had actually bound to SSTRs, and was not washed out. There is some evidence from animal studies suggesting that isolated hepatic Kupffer cells express SSTRs [39]. It is also possible that the SSTR expression in various liver cells increased due to inflammatory processes caused by the surgical procedure, or that cells in the bile ducts in the liver might express SSTRs [37].

It should be mentioned that one limitation of the study is that the activity concentration during the IHP and rinsing was only measured at one position with the IGD, with a relatively narrow field-of-view (FOV). The reason was to avoid uncertainties due to positioning in this part of the study where focus was on biokinetics in the liver. It should also be mentioned that the leakage we had in this *ex vivo* situation would not occur, or be much less, in the *in vivo* situation.

The SPECT images revealed a relatively inhomogeneous distribution of ^{177}Lu in the liver. As mentioned above, one reason for this could be inhomogeneous perfusion within the liver or differences in regional perfusion when adding ^{177}Lu-octreotate and rinsing fluid. The highest uptake regions appeared to be close to the large vessels in the liver. Excluding this relatively small highest-uptake region (red/white in Fig. 5) and also the voxels outside or close to the edge of the liver (blue in Fig. 5, probably affected by a substantial amount of partial-volume effect), it can be seen that the variation in the vast majority of the liver tissue was within a factor of about 2 (i.e. green (ca. 30%) to yellow (ca. 60%) in Fig. 5).

The inhomogeneity revealed by the SPECT images was also seen in the 50 biopsies. According to the CV values (77% in the SPECT image *vs.* 36% in the biopsies), the variation was lower in the biopsies than in the SPECT image voxels, most probably due to the larger subregion analysed (about 1000 mm^3 biopsy *vs.* the SPECT voxel size of *ca.* 86 mm^3), and more similar tissue content, avoiding large vessels. The opposite was seen in the SEM/mean values (0.53% in the SPECT *vs.* 5.1% in the biopsies), which can be explained by the huge difference in number of samples (21087 SPECT voxels *vs.* 50 biopsies). Given the inhomogeneity obtained, it would be important to measure activity concentration at many different positions over the liver *in vivo* if this procedure were used for patients, to be able to more accurately determine activity concentration using an IGD.

The activity concentration values obtained with the IGD showed altogether an acceptable agreement (statistically significant correlation) with the corresponding values in the biopsies sampled directly underneath each IGD measurement position, although discrepancies were seen in individual values. Higher C_{IGD}/C_B values were seen for larger liver thicknesses despite that the translation from measured count rate to activity concentration included correction for differences

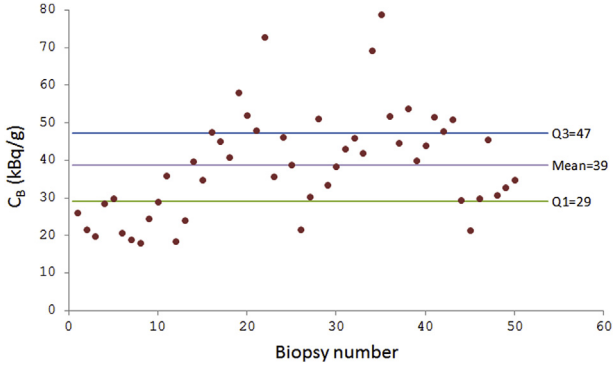

Fig. 6. The ^{177}Lu activity concentration in the 50 biopsies taken from the liver. Lines corresponding to the first quartile (Q1), mean and third quartile (Q3) are included [single-column fitting image].

in thickness. The reason could be that the biopsies were collected close to the surface of the liver, with possibly lower activity concentration (shown by SPECT), whereas the IGD collected photons from the entire volume inside its FOV (*i.e.* also from ^{177}Lu in deeper regions, although at lower efficiency of the detector) and the thickness correction assumed homogeneous activity distribution with depth. Theoretically, this difference would be more apparent at thicker liver regions where also the larger vessels are located, which is also seen in the results.

For a clinical procedure, where ^{177}Lu-octreotate is locally administered to the liver via IHP, it is important to accurately determine the activity concentration in normal liver and to estimate absorbed dose. This determination may be influenced by the much higher activity concentration in metastatic tissue. Liver metastases from NETs appear in various geometrical forms, from multiple very small tumours in a large part of the liver to a single or few larger tumours. This must be considered in practice to ensure optimal measurements in order to determine the absorbed dose to normal liver as accurately as possible. Also the absorbed dose to tumours is of high importance when implementing this new treatment technique, as well as other organs that might take up a certain amount of ^{177}Lu-octreotate after the systemic circulation has been re-established after the IHP procedure.

To be able to estimate absorbed dose based on a measured activity concentration in a clinical situation, information about radionuclide biokinetics, absorbed fractions and organ masses are needed. Determination of activity concentration both during and after IHP is important as this will affect the absorbed dose. During the IHP, when the liver contains a large amount of radioactive blood (or radioactivity that will be washed out during the rinsing), repeated measurements with an IGD could be used to estimate activity concentration. Based on the variation in the C_{IGD}/C_B values in this study, the uncertainty in determining activity concertation with an IGD at a given position at the surface of the liver is about ± 50%. For estimation of activity concentration after the IHP, a gamma camera could be used to scan the patient at certain time points (*e.g.* day 7 and 14), depending on the health status of the patient. We have previously shown that the biological half-life of ^{177}Lu-octreotate in liver tissue including metastases from NETs is about 4.5 days [40]. Furthermore, the general biokinetics of ^{111}In-octreotide is similar to that of ^{177}Lu-octreotate, and we have shown that the biological half-life of ^{111}In-octreotide is about 4.0 days and 1.7 days for liver with and without metastases from NETs present, respectively [41].

In this *ex vivo* simulation, the liver was rinsed for about 50 min. In a clinical situation, the liver would become ischemic with such a long rinsing time. During our standard IHP procedure to treat patients with liver metastases from melanoma, the liver is perfused for 60 min with a perfusate containing blood and the chemotherapeutic agent melphalan, and the blood ensures a normal oxygenation of the liver throughout the procedure. When the perfusion is finished, the liver is rinsed with 1000–2000 ml of Ringer's solution which takes about 5–10 min. In this study, a fast decrease in count rate was experienced after the rinsing was started, and after 10 min, a large part of the ^{177}Lu-octreotate had been washed out. However, in the present study, we wanted to investigate if more ^{177}Lu-octreotate could be washed out with an increased rinsing time. As can be seen in the results, the count rate reached a plateau after about 10–20 min, after which only a small decrease in count rate was experienced. Therefore, we believe that the standard rinsing with 1000–2000 ml of Ringer's solution is appropriate also for IHP with ^{177}Lu-octreotate.

In total, if an IGD would be used to determine activity concentration *in vivo*, the uncertainty in a calculated absorbed dose for tumour or healthy liver tissue for this type of procedure would be about ± 60%. This number was estimated assuming that the individual uncertainties (*e.g.* uncertainty in the calibration of the IGD, uncertainty in the liver thickness estimation, etc.) were independent of each other [42]. Based on the inhomogeneous distribution in healthy liver tissue seen in this study, some parts of the liver could receive much higher doses than the calculated mean value for the entire liver.

In a clinical situation, staff members can be positioned close to the patient during at least part of the IHP. This could potentially pose a radiation protection problem if ^{177}Lu-octreotate is used. In Sweden, the dose limit for staff working with ionising radiation is 20 mSv/year for whole body exposure ($H_p(10)$) and 500 mSv/year for extremity exposure ($H_p(0.07)$) [43]. During the IHP in this study, all staff members could be positioned behind shielding equipment almost throughout the entire perfusion, and therefore, no measureable radiation doses were recorded by the personal dosimeters. The same is possible in a clinical situation. However, after the perfusion and rinsing is finished, the surgeon will have to remove all tubes, reconnect blood vessels, and close the surgical field, something that was not required in this study. This part of the surgery requires the surgeon to stand close to the patient for about 60 min. Based on the ambient equivalent dose rate measured at 20 cm from the liver in this study, and assuming that 75% of the activity will be washed out during the rinsing, but also that the administered activity could be about 10 times higher in a patient situation compared with the present experiment, a surgeon should be able to perform about 800 procedures before exceeding the annual dose limit for whole body exposure, *i.e.* a situation that is not clinically realistic. Other factors that would influence the dose rate to staff compared with the present experiment are the following. Firstly, if the liver would have contained tumours, in which a high uptake of ^{177}Lu is expected, the dose rate for the staff could have been somewhat increased. Secondly, this experiment was carried out *ex vivo*, which means that the photons emitted from the liver were not shielded by a patient's body, something that would have reduced the dose rate. Altogether, the occupational radiation protection in a clinical situation has to be closely monitored, but is not expected to be of any problem in practice. For comparison, the effective dose for medical staff involved in systemic ^{177}Lu-octreotate therapy is about 10–30 μSv per treatment day corresponding to 0.25–0.75 mSv per year [44].

Patients undergoing this type of treatment would probably have to receive post-operative care at an intensive care unit for about 24 h, where both staff members but also other patients are in relatively close proximity of the ^{177}Lu-treated patient, followed by care at a surgical ward in a single room for about 1 week. Assuming that the same staff members will tend to the patient during this time, a staff member would receive an effective dose of about 0.6 mSv, standing 50 cm from the patient, 8 h per day, for 1 week (as a worst case scenario). While this is a reasonably low effective dose, the ALARA principle (as low as reasonably achievable) should be adopted, for example by placing a protective lead screen between the patient and the staff member. The exposure of other patients would be even lower due to the larger distance between them (approximately 3 m), and due to the shorter time spent in the same room. Therefore, this exposure should not pose a problem, especially if protective lead screens are placed between the patients.

5. Conclusions

Altogether, the results show that it could be feasible to treat patients with liver metastases from NETs with ^{177}Lu-octreotate via IHP. To account for a potentially inhomogeneous distribution of ^{177}Lu-octreotate in normal liver tissue, measurements using an intraoperative gamma detector need to be performed at several positions over the liver to be able to determine the activity concentration with satisfactory accuracy. Furthermore, we find that the radiation exposure of the staff and patients in the ward can clearly be kept below regulatory dose limits if appropriate radiation protection measures are taken. To proceed towards clinical use, the treatment situation must be further simulated to ensure that dosimetric and radiobiological prerequisites are met for tumour and normal tissues.

Declarations of interest

None.

Authors' contributions

Study planning was collectively carried out by all authors. The IHP was performed by CH and ROB. Data acquisition during and after IHP was performed by VS and IS. Data analysis was performed by VS and IS. VS drafted the first version of the manuscript. All authors read and revised the manuscript, and approved the final version.

Ethics approval

All applicable national and institutional guidelines for the care and use of animals were followed. This study was approved by the Ethical Committee on Animal Experiments in Gothenburg, Sweden.

Data statement

The datasets used and/or analysed during the current study are available from the corresponding author on reasonable request.

6 Acknowledgements

The authors thank Tobias Rydén, Rebecca Hermann, and Linn Hagmarker for their assistance with the SPECT/CT imaging and analysis. This study was supported by the Swedish Research Council (grant no. 21073), the Swedish Cancer Society (grant no. 3427), BioCARE – a National Strategic Research Program at the University of Gothenburg, the Swedish state under the agreement between the Swedish government and the county councils – the ALF-agreement (ALFGBG-725031), the Knut and Alice Wallenberg Foundation, the King Gustav V Jubilee Clinic Cancer Research Foundation, the Sahlgrenska University Hospital Research Funds, the Assar Gabrielsson Cancer Research Foundation, the Adlerbertska Research Foundation, and the Wilhelm and Martina Lundgren Science Fund.

Appendix A. Supplementary data

Supplementary data to this article can be found online at https://doi.org/10.1016/j.suronc.2019.05.002.

References

[1] S. Massironi, V. Sciola, M. Peracchi, C. Ciafardini, M.P. Spampatti, D. Conte, Neuroendocrine tumors of the gastro-entero-pancreatic system, World J. Gastroenterol. 35 (2008) 5377–5384 https://doi.org/10.3748/wjg.14.5377.

[2] J.C. Yao, M. Hassan, A. Phan, C. Dagohoy, C. Leary, J.E. Mares, et al., One hundred years after "carcinoid": epidemiology of and prognostic factors for neuroendocrine tumors in 35,825 cases in the United States, J. Clin. Oncol. 18 (2008) 3063–3072 https://doi.org/10.1200/JCO.2007.15.4377.

[3] A.I. Vinik, E.A. Woltering, R.R. Warner, M. Caplin, T.M. O'Dorisio, G.A. Wiseman, et al., NANETS consensus guidelines for the diagnosis of neuroendocrine tumor, Pancreas 6 (2010) 713–734 https://doi.org/10.1097/MPA.0b013e3181ebaffd.

[4] I.M. Modlin, K.D. Lye, M. Kidd, A 5-decade analysis of 13,715 carcinoid tumors, Cancer 4 (2003) 934–959 https://doi.org/10.1002/cncr.11105.

[5] I.M. Modlin, M.C. Champaneria, A.K. Chan, M. Kidd, A three-decade analysis of 3,911 small intestinal neuroendocrine tumors: the rapid pace of no progress, Am. J. Gastroenterol. 7 (2007) 1464–1473 https://doi.org/10.1111/j.1572-0241.2007.01185.x.

[6] T.R. Halfdanarson, J. Rubin, M.B. Farnell, C.S. Grant, G.M. Petersen, Pancreatic endocrine neoplasms: epidemiology and prognosis of pancreatic endocrine tumors, Endocr. Relat. Cancer 2 (2008) 409–427 https://doi.org/10.1677/ERC-07-0221.

[7] O. Hauso, B.I. Gustafsson, M. Kidd, H.L. Waldum, I. Drozdov, A.K. Chan, et al., Neuroendocrine tumor epidemiology, Cancer 10 (2008) 2655–2664 https://doi.org/10.1002/cncr.23883.

[8] B. Lawrence, B.I. Gustafsson, A. Chan, B. Svejda, M. Kidd, I.M. Modlin, The epidemiology of gastroenteropancreatic neuroendocrine tumors, Endocrinol Metab. Clin. N. Am. 1 (2011) 1–18 https://doi.org/10.1016/j.ecl.2010.12.005.

[9] M. Olausson, S. Friman, G. Herlenius, C. Cahlin, O. Nilsson, S. Jansson, et al., Orthotopic liver or multivisceral transplantation as treatment of metastatic neuroendocrine tumors, Liver Transplant. 3 (2007) 327–333 https://doi.org/10.1002/lt.21056.

[10] B.I. Gustafsson, M. Kidd, I.M. Modlin, Neuroendocrine tumors of the diffuse neuroendocrine system, Curr. Opin. Oncol. 1 (2008) 1–12 https://doi.org/10.1097/CCO.0b013e3282f1c595.

[11] G.A. Kaltsas, G.M. Besser, A.B. Grossman, The diagnosis and medical management of advanced neuroendocrine tumors, Endocr. Rev. 3 (2004) 458–511 https://doi.org/10.1210/er.2003-0014.

[12] I.M. Modlin, K. Oberg, D.C. Chung, R.T. Jensen, W.W. de Herder, R.V. Thakker, et al., Gastroenteropancreatic neuroendocrine tumours, Lancet Oncol. 1 (2008) 61–72 https://doi.org/10.1016/S1470-2045(07)70410-2.

[13] T. De Baere, F. Deschamps, L. Tselikas, M. Ducreux, D. Planchard, E. Pearson, et al., GEP-NETS UPDATE: interventional radiology: role in the treatment of liver metastases from GEP-NETs, Eur. J. Endocrinol. 4 (2015) R151–R166 https://doi.org/10.1530/EJE-14-0630.

[14] D.J. Kwekkeboom, W.W. de Herder, B.L. Kam, C.H. van Eijck, M. van Essen, P.P. Kooij, et al., Treatment with the radiolabeled somatostatin analog [177Lu-DOTA0, Tyr3] octreotate: toxicity, efficacy, and survival, J. Clin. Oncol. 13 (2008) 2124–2130 https://doi.org/10.1200/JCO.2007.15.2553.

[15] M. Gabriel, U. Andergassen, D. Putzer, A. Kroiss, D. Waitz, E. von Guggenberg, et al., Individualized peptide-related-radionuclide-therapy concept using different radiolabelled somatostatin analogs in advanced cancer patients, Q. J. Nucl. Med. Mol. Imag. 1 (2010) 92–99.

[16] C. Swärd, P. Bernhardt, H. Ahlman, B. Wängberg, E. Forssell-Aronsson, M. Larsson, et al., [177Lu-DOTA0-Tyr3]-octreotate treatment in patients with disseminated gastroenteropancreatic neuroendocrine tumors: the value of measuring absorbed dose to the kidney, World J. Surg. 6 (2010) 1368–1372 https://doi.org/10.1007/s00268-009-0387-6.

[17] P.G. Claringbold, P.A. Brayshaw, R.A. Price, J.H. Turner, Phase II study of radiopeptide 177Lu-octreotate and capecitabine therapy of progressive disseminated neuroendocrine tumours, Eur. J. Nucl. Med. Mol. Imaging 2 (2011) 302–311 https://doi.org/10.1007/s00259-010-1631-x.

[18] J. Svensson, J. Mölne, E. Forssell-Aronsson, M. Konijnenberg, P. Bernhardt, Nephrotoxicity profiles and threshold dose values for 177Lu-DOTATATE in nude mice, Nucl. Med. Biol. 6 (2012) 756–762 https://doi.org/10.1016/j.nucmedbio.2012.02.003.

[19] L. Bodei, M. Kidd, G. Paganelli, C.M. Grana, I. Drozdov, M. Cremonesi, et al., Long-term tolerability of PRRT in 807 patients with neuroendocrine tumours: the value and limitations of clinical factors, Eur. J. Nucl. Med. Mol. Imaging 1 (2015) 5–19 https://doi.org/10.1007/s00259-014-2893-5.

[20] E. Forssell-Aronsson, J. Spetz, H. Ahlman, Radionuclide therapy via SSTR: future aspects from experimental animal studies, Neuroendocrinology 1 (2013) 86–98 https://doi.org/10.1159/000336086.

[21] M. Rizell, J. Mattson, C. Cahlin, L. Hafström, P. Lindner, M. Olausson, Isolated hepatic perfusion for liver metastases of malignant melanoma, Melanoma Res. 2 (2008) 120–126 https://doi.org/10.1097/CMR.0b013e3282f8e3c9.

[22] R. Olofsson, C. Cahlin, C. All-Ericsson, F. Hashimi, J. Mattsson, M. Rizell, et al., Isolated hepatic perfusion for ocular melanoma metastasis: registry data suggests a survival benefit, Ann. Surg. Oncol. 2 (2014) 466–472 https://doi.org/10.1245/s10434-013-3304-z.

[23] I. Ben-Shabat, C. Hansson, M.S. Eilard, C. Cahlin, M. Rizell, P. Lindnér, et al., Isolated hepatic perfusion as a treatment for liver metastases of uveal melanoma, JoVE (Journal of Visualized Experiments) 95 (2015) e52490 e52490 https://doi.org/10.3791/52490.

[24] D.L. Bartlett, S.K. Libutti, W.D. Figg, D.L. Fraker, H.R. Alexander, Isolated hepatic perfusion for unresectable hepatic metastases from colorectal cancer, Surgery 2 (2001) 176–187 https://doi.org/10.1067/msy.2001.110365.

[25] A.C. Grover, S.K. Libutti, J.F. Pingpank, C. Helsabeck, T. Beresnev, H.R. Alexander Jr., Isolated hepatic perfusion for the treatment of patients with advanced liver metastases from pancreatic and gastrointestinal neuroendocrine neoplasms, Surgery 6 (2004) 1176–1182 https://doi.org/10.1016/j.surg.2004.06.044.

[26] V. Sandblom, I. Ståhl, R. Olofsson Bagge, E. Forssell-Aronsson, Evaluation of two intraoperative gamma detectors for assessment of ^{177}Lu activity concentration in vivo, EJNMMI Physics 1 (2017) 3 https://doi.org/10.1186/s40658-016-0168-x.

[27] S.P. Povoski, R.L. Neff, C.M. Mojzisik, D.M. O'Malley, G.H. Hinkle, N.C. Hall, et al., A comprehensive overview of radioguided surgery using gamma detection probe technology, World J. Surg. Oncol. 1 (2009) 11 https://doi.org/10.1186/1477-7819-7-11.

[28] H. Ahlman, L. Tisell, B. Wängberg, O. Nilsson, M. Fjälling, E. Forssell-Aronsson, Somatostatin receptors on neuroendocrine tumors - a way to intraoperative diagnosis and localization, Yale J. Biol. Med. 3–4 (1994) 215–221.

[29] B. Wängberg, E. Forssell-Aronsson, L. Tisell, O. Nilsson, M. Fjälling, H. Ahlman, Intraoperative detection of somatostatin-receptor-positive neuroendocrine tumours using indium-111-labelled DTPA-D-Phe1-octreotide, Br. J. Canc. 6 (1996) 770–775.

[30] S.A. Benjegård, E. Forssell-Aronsson, B. Wängberg, J. Skånberg, O. Nilsson, H. Ahlman, Intraoperative tumour detection using 111In-DTPA-D-Phe1-octreotide and a scintillation detector, Eur. J. Nucl. Med. 10 (2001) 1456–1462 https://doi.org/10.1007/s002590100600.

[31] J. Skånberg, H. Ahlman, S.A. Benjegård, M. Fjälling, E. Forssell-Aronsson, S.H. Hashemi, et al., Indium-111-octreotide scintigraphy, intraoperative gamma-detector localisation and somatostatin receptor expression in primary human breast cancer, Breast Canc. Res. Treat. 2 (2002) 101–111.

[32] D. Krag, D. Weaver, J. Alex, J. Fairbank, Surgical resection and radiolocalization of the sentinel lymph node in breast cancer using a gamma probe, Surg. Oncol. 6 (1993) 335–340 https://doi.org/10.1016/0960-7404(93)90064-6.

[33] M.D. McCarter, H. Yeung, S. Yeh, J. Fey, P.I. Borgen, H.S. Cody III, Localization of

the sentinel node in breast cancer: identical results with same-day and day-before isotope injection, Ann. Surg. Oncol. 8 (2001) 682–686.
[34] Nuclear Decay Data in the MIRD Format, National Nuclear Data Center, 2003, http://www.nndc.bnl.gov/mird/ , Accessed date: 14 November 2017accessed.
[35] A. Kennedy, L. Bester, R. Salem, R.A. Sharma, R.W. Parks, P. Ruszniewski, Role of Hepatic Intra-arterial Therapies in Metastatic Neuroendocrine Tumours (NET): Guidelines from the NET-Liver-Metastases Consensus Conference, HPB, vol. 1, 2015, pp. 29–37 https://doi.org/10.1111/hpb.12326.
[36] M.K. McStay, D. Maudgil, M. Williams, J.M. Tibballs, A.F. Watkinson, M.E. Caplin, et al., Large-volume liver metastases from neuroendocrine tumors: hepatic intraarterial 90Y-DOTA-lanreotide as effective palliative therapy, Radiology 2 (2005) 718–726 https://doi.org/10.1148/radiol.2372041203.
[37] H. Reynaert, K. Rombouts, A. Vandermonde, D. Urbain, U. Kumar, P. Bioulac-Sage, et al., Expression of somatostatin receptors in normal and cirrhotic human liver and in hepatocellular carcinoma, Gut 8 (2004) 1180–1189 https://doi.org/10.1136/gut.2003.036053.
[38] R. Olofsson, J. Mattsson, P. Lindnér, Long-term follow-up of 163 consecutive patients treated with isolated limb perfusion for in-transit metastases of malignant melanoma, Int. J. Hyperth. 6 (2013) 551–557 https://doi.org/10.3109/02656736.2013.802374.
[39] C. Xidakis, N. Mastrodimou, G. Notas, E. Renieri, G. Kolios, E. Kouroumalis, et al., RT-PCR and immunocytochemistry studies support the presence of somatostatin, cortistatin and somatostatin receptor subtypes in rat Kupffer cells, Regul. Pept. 1 (2007) 76–82 https://doi.org/10.1016/j.regpep.2007.03.005.
[40] M. Larsson, Therapy with ^{177}Lu-Octreotate – Pharmacokinetics, Dosimetry and Kidney Toxicity [PhD Thesis], University of Gothenburg, Sweden, 2014http://hdl.handle.net/2077/35451.
[41] E. Forssell-Aronsson, B. Lanhede, M. Fjälling, B. Wängberg, L. Tisell, H. Ahlman, et al., Pharmacokinetics and dosimetry of ^{111}In-DTPA-D-Phe^{1}-octreotide in patients with neuroendocrine tumors, sixth international radiopharmaceutical dosimetry symposium, Proceedings of a Conference held at Gatlinburg, Tennessee, May 7-10, 1996, 99–0164 1999, pp. 643–654 (Edited by A Schlafke-Stelson and EE Watson), ORISE.
[42] JCGM 100, Evaluation of Measurement Data – Guide to the Expression of Uncertainty in Measurement, Joint Committee for Guides in Metrology, (2008).
[43] SFS 2018:506. Dose Limits in Practices Involving Ionising Radiation, Swedish Code of Statutes 2§, 2018.
[44] P.J. Calais, J.H. Turner, Radiation safety of outpatient 177Lu-octreotate radiopeptide therapy of neuroendocrine tumors, Ann. Nucl. Med. 6 (2014) 531–539 https://doi.org/10.1007/s12149-014-0843-8.